

# Synthesis and Characterization of Suspension-Polymerized Poly(vinyl Alcohol) Beads with Core-Shell Structure

CHERNG-JU KIM<sup>1</sup> and PING I. LEE<sup>1,2,\*</sup>

<sup>1</sup>Faculty of Pharmacy, and <sup>2</sup>Department of Chemical Engineering and Applied Chemistry, University of Toronto, Toronto, Ontario, Canada M5S 2S2

## SYNOPSIS

A new method of preparing large spherical PVA beads (up to 1.5 mm diameter) with a core-shell structure has been developed. This involves a stepwise saponification of suspension polymerized PVAc beads, followed by a stepwise crosslinking of the PVA core and shell with glutaraldehyde. The resulting composite PVA beads have thin, highly crosslinked outer shells and lightly to moderately crosslinked inner cores of different degrees of crosslinking. In addition to the characterization of structural parameters, the kinetics of solute release and the swelling dynamics, including the transient dimensional changes, have been investigated using proxiphylline as a model compound. © 1992 John Wiley & Sons, Inc.

## INTRODUCTION

Crosslinked hydrophilic polymers have found extensive application, ranging from separations<sup>1</sup> and superabsorbent materials<sup>2</sup> to controlled-release drug delivery.<sup>3</sup> Available in various physical forms, such as powders, granules, or beads, these polymers are generally glassy in the dehydrated state, but swell to become an elastic gel upon water penetration. In drug delivery applications, when such swelling takes place in a glassy matrix containing the dissolved or dispersed drug, the entrapped drug concomitantly dissolves and diffuses through the swollen network into the surrounding aqueous medium. The rate of drug release from such swelling-controlled systems is strongly affected by the relative contributions of the macromolecular relaxation process vs. the drug diffusion process.<sup>4</sup> When the former process is rate-limiting, the release kinetics may deviate from the inherent, first-order Fickian behavior and may approach linear kinetics. Typically, the cross-linking density and the water swelling are further regulated to control the rate of drug release from such crosslinked hydrophilic polymers.<sup>5</sup>

Poly(vinyl alcohol) (PVA) has been investigated as a drug carrier for controlled-release applica-

tions.<sup>6,7</sup> Frequently, the hydrophilic PVA network is modified by crosslinking to reduce the volume swelling and the rate of drug release. This is accomplished through a reduction in the mol wt between crosslinks and the associated macromolecular mesh sizes,<sup>5</sup> thereby resulting in a decrease in diffusion coefficients for both the drug and the swelling solvent. The crosslinking is preferably carried out before the drug loading process to avoid possible side-reactions between the drug and crosslinking agent.

Despite the growing interest in utilizing glassy PVA hydrogels as swelling-controlled drug delivery systems, the kinetics of the swelling of crosslinked PVA hydrogels during solute release has not been investigated in detail, primarily due to limitations on available sample geometry. For example, reliable swelling data are difficult to obtain from commonly employed disc or granular samples, due to the well-known anisotropic swelling behavior, the edge effect, and technical difficulties in the direct observation of swelling front penetrations. On the other hand, spherical geometry avoids these drawbacks by virtue of its radial symmetry and, thereby, permits accurate measurement of the swelling front penetration and transient dimensional changes during solute release. This aspect is important in the elucidation of swelling mechanisms in other hydrogel systems.<sup>8,9</sup>

This article describes a new method of preparation of large spherical PVA beads (up to 1.5 mm

\* To whom correspondence should be addressed.

diameter) with a core-shell structure from suspension polymerized poly(vinyl acetate) (PVAc). A preliminary report on the preparation of such composite beads for drug delivery applications has been given elsewhere.<sup>10</sup> Here, we present details on the synthesis and characterization of swelling kinetics of such double-layered composite PVA beads.

## EXPERIMENTAL

### Materials

Reagent-grade vinyl acetate (Fisher Scientific) was vacuum distilled using cuprous chloride as inhibitor. Other chemicals were all reagent-grade and were used as received without further purification.

### Synthesis of PVAc Beads

The suspension polymerization of vinyl acetate was carried out in an aqueous medium containing 1.0 wt % of fully hydrolyzed PVA (MW 106,000–110,000, Aldrich Chemical) as suspending agent and 0.5 wt % of AIBN (Vazo 64, DuPont) as initiator. The relative amount of vinyl acetate to water in the polymerization mixture was 1 : 5 by weight. The polymerization was carried out in a 2 L reaction flask at 60–65°C and 150 rpm for 5–6 h. The reaction mixture was filtered and washed with hot water to remove residual PVA suspending agent. The PVAc beads so recovered were extracted with methanol/water mixtures for three days before being dried. These dry PVAc beads were subsequently processed in a stepwise fashion, as described below, to obtain the desired PVA gel beads.

### Conversion to PVA Gel Beads

Partially converted PVAc beads, consisting of an outer PVA shell and an inner PVAc core, were prepared by a partial saponification of PVAc beads in a 35% aqueous solution of NaOH/Na<sub>2</sub>SO<sub>4</sub>/methanol (2 : 1 : 1 by weight) at 60°C for 4 h to produce a saponified surface layer of about 10% of the original radius. The PVA shell of such partially converted PVAc beads was subsequently crosslinked with glutaraldehyde at 60°C for 2 h in an excess of aqueous solution containing 2% glutaraldehyde, 5% acetic acid/methanol (1 : 2 by wt), 10% Na<sub>2</sub>SO<sub>4</sub>, and 0.04% of H<sub>2</sub>SO<sub>4</sub> as catalyst. Intermediate PVA beads (designated as PVA I), consisting of an outer crosslinked PVA shell and an inner uncrosslinked PVA core, were subsequently prepared by a complete

saponification of the remaining PVAc core in a 45% aqueous solution of NaOH/Na<sub>2</sub>SO<sub>4</sub>/methanol (2 : 1 : 5 by wt) at 60°C for 5 h.

The resulting PVA I beads were then subjected to additional crosslinking in an acidic methanolic solution of glutaraldehyde, similar to that described above but with varying glutaraldehyde concentrations, to produce PVA beads (designated as PVA II) having highly crosslinked outer shells and lightly to moderately crosslinked inner cores. A range of crosslinking density was obtained by varying the initial concentration of glutaraldehyde to achieve the desired crosslinking ratio  $X$ , defined as the number of moles of glutaraldehyde per moles of repeating vinyl alcohol units in PVA. The resulting PVA II beads were soaked in water for three days to remove any extractables before being dried at room temperature under vacuum for further study. In the following sections,  $X_c$  will represent the crosslinking ratios of the PVA core and  $X_s$  for that of the PVA shell.

### Swelling and Diffusion Experiments

Proxiphylline (water solubility of approx. 50%) was selected as a model compound for the characterization of swelling and transient dimensional changes in PVA beads. Different solute loading levels in PVA I and PVA II were achieved by equilibrating PVA beads in concentrated aqueous proxiphylline solutions at 37°C for four days. After filtering, rinsing, and drying, proxiphylline-loaded beads, with a size range of about 0.9–1 mm diameter, were used for subsequent swelling and diffusion studies in distilled/deionized water. The amount of proxiphylline loading was determined spectrophotometrically after a complete extraction of solute-loaded beads in water. The swelling experiments were performed in a water-jacketed cuvette, maintained at 37°C, with a circulating water bath. The swelling front movement and transient dimensional change were observed with a WILD M420 stereomicroscope, equipped with a digital length-measuring unit (MMS 235). The proxiphylline diffusion at 37°C, under perfect sink condition, was monitored continuously at 260 nm in a stirred cuvette on a Hewlett-Packard 8452A diode-array UV-Vis spectrophotometer, equipped with a water-jacketed cuvette holder and a built-in magnetic stirrer.

### Determination of PVA Molecular Weight

The mol wt,  $M$ , of PVA was determined from the intrinsic viscosity,  $[\eta]$ , of reacetylated PVA in ace-

tone at 30°C according to the following Mark-Houwink-Sakurada equation<sup>11</sup>:

$$[\eta] = 1.2 \times 10^{-4} M^{0.72} \quad (1)$$

The reacetylation of PVA was carried out by reacting 5 g of uncrosslinked PVA (from fully saponified PVAc beads) with a mixture of 10 mL of pyridine, 100 mL of acetic anhydride, and 1000 mL of acetic acid in a stirred reaction flask at 100°C for 24 h under nitrogen. The resulting PVAc was precipitated in water, washed with methanol/water mixtures, and dried under vacuum at 60°C. The mol wt of PVAc was then determined from the intrinsic viscosity data obtained on a Ubbelohde viscometer. The mol wt of PVA is taken to be equal to that of the corresponding reacetylated PVA.

## RESULTS AND DISCUSSION

### Preparation of Composite PVA Beads

The PVAc beads, synthesized via suspension polymerization, were spherical and smooth, with diameters up to 1.5 mm. Figure 1(a) is a photograph showing a typical batch of PVAc beads synthesized in the present study. The corresponding average particle size distribution is shown in Figure 1(b). The normal synthetic procedure in converting PVAc to PVA generally involves the alkali or acid hydrolysis of PVAc in an alcohol solution.<sup>12</sup> During such a direct reaction, PVAc in the solution phase is rapidly hydrolyzed to PVA with concomitant precipitation in the alcohol solution. However, in order to preserve the spherical shape of PVA beads for the

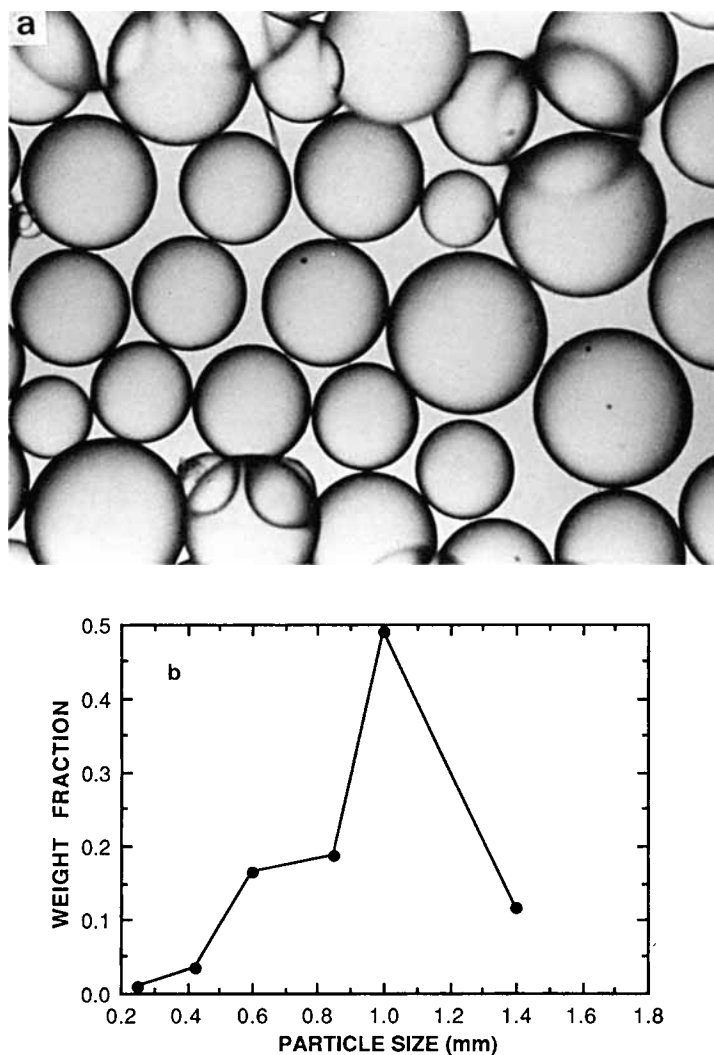


**Figure 1** A typical batch of suspension polymerized PVAc beads (a) photograph, (b) particle size distribution.

purpose of the present study, it was not feasible to hydrolyze the PVAc beads directly, due to the lack of structural rigidity and the gradual dissolution of formed PVA in the saponifying medium. To overcome this difficulty, a process involving stepwise saponification with subsequent stepwise crosslinking was developed in the present study. A schematic diagram showing the reaction steps involved is presented in Figure 2. This is a modification of the process reported by Hirayama et al.<sup>13</sup> for preparing micron-sized PVA particles as column packing materials for size exclusion chromatography.

In the first step of the process, PVAc beads were saponified mainly on the surface in an alkaline methanolic solution (see Experimental). The reaction time and methanol concentration were controlled, such that the thickness of the saponified surface layer was about 10% of the original bead radius. This was achieved by frequent microscopic examination of the reaction front penetration during saponification and by keeping the methanol con-

centration in the saponifying medium below 10%. The low concentration of methanol was necessary to slow the reaction front penetration since the saponification of PVAc was rapid at high concentrations of methanol. At this point, the integrity of these beads was provided by the remaining PVAc core. The swollen PVA surface layer was prevented from dissolving by a high concentration of  $\text{Na}_2\text{SO}_4$  in the saponifying medium. Figure 3 is a photograph of these PVA beads during surface saponification, showing an outer, uncrosslinked PVA shell (clear) and an inner PVAc core (dark). Although PVAc beads appear to be clear before modification [Fig. 1(a)], the slight opaqueness of the PVAc core during saponification is probably caused by the precipitation of freshly formed PVA at the surface of the PVAc core, where the methanol concentration is expected to be somewhat higher than that in the rest of the PVA shell, due to preferential sorption of methanol in PVAc. During the subsequent glutaraldehyde crosslinking of such a PVA surface

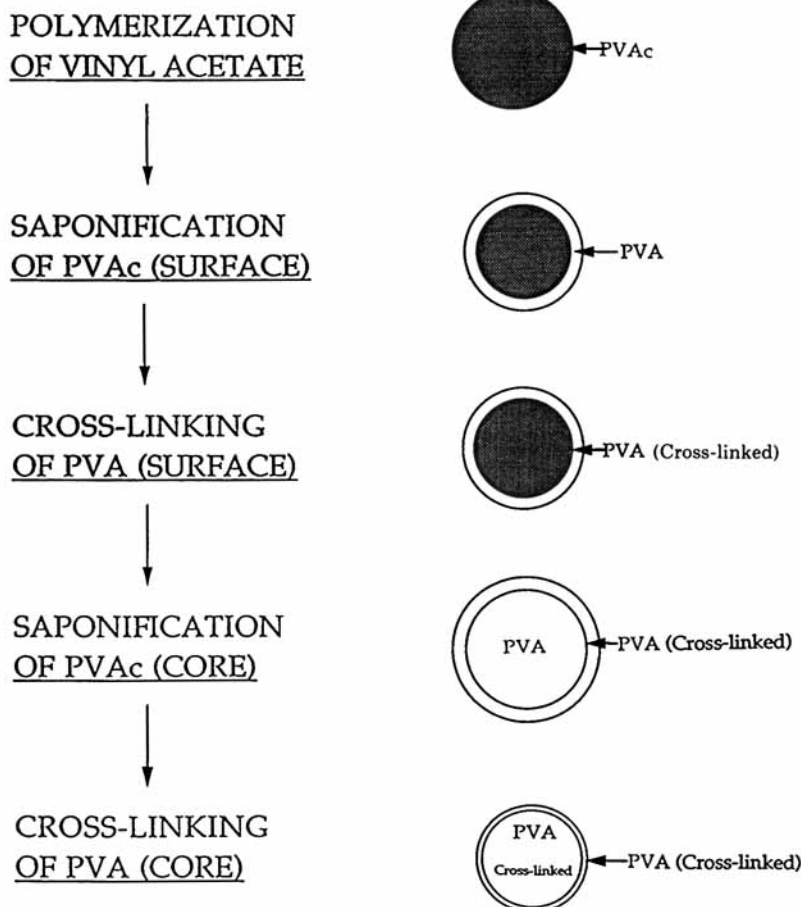


**Figure 2** Schematic diagram of reaction steps involved in the preparation of composite PVA beads.

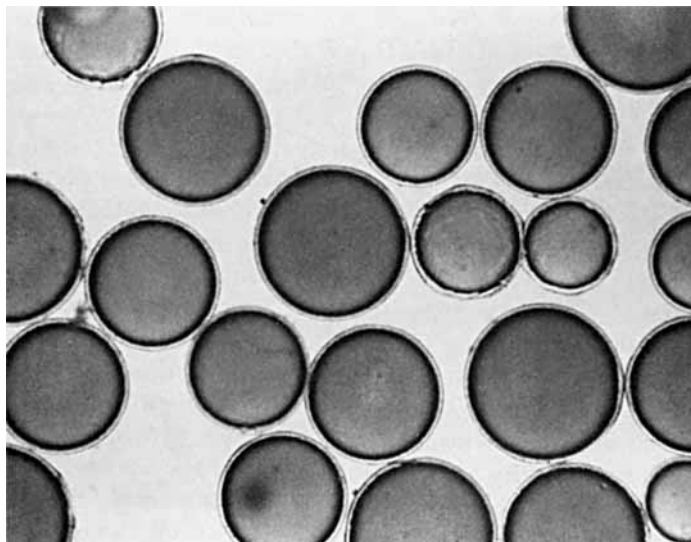


**Figure 3** Photograph of a typical batch of PVAc beads during surface saponification.

layer, a reduction in the thickness of the swollen PVA shell from 10% to about 5% of the bead radius was observed. Here, a shell crosslinking ratio  $X_s \approx 0.3$  was estimated from swelling measurement.<sup>10</sup> This crosslinked PVA shell provided structural support for the PVA gel core in PVA I, which was formed by completely saponifying the remaining PVAc core. Figure 4 shows a typical batch of partially saponified PVAc beads observed during the last step of conversion into PVA I, where the opaque and shrinking PVAc core is separated from the thin,

crosslinked PVA shell by a clear intermediate region of uncrosslinked PVA gel.

Further crosslinking of PVA I with glutaraldehyde resulted in PVA II beads having a composite structure of a highly crosslinked outer shell and a lightly to moderately crosslinked inner core. During such a crosslinking process, a further reduction of the outer shell thickness took place, resulting in an average swollen shell thickness of about 21  $\mu\text{m}$  in PVA II. For ease of identification, the crosslinking ratio of the shell of PVA II has been taken to be the

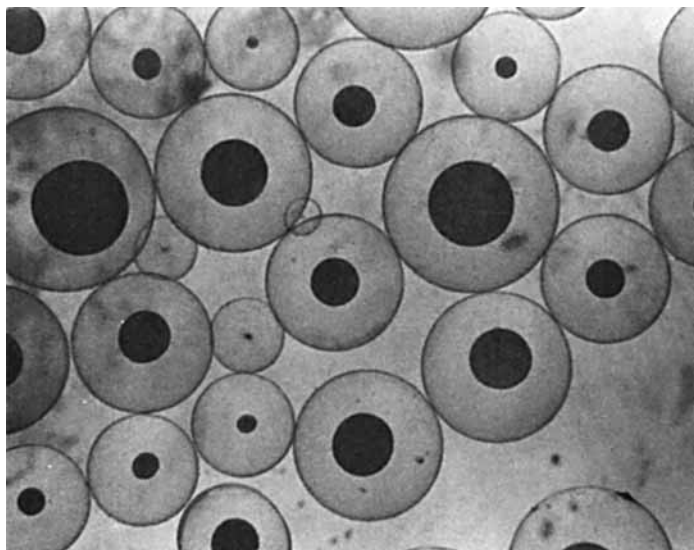


**Figure 4** Photograph showing a typical batch of partially saponified PVAc beads during the last step of conversion into PVA I.

sum of the shell crosslinking ratio of PVA I, 0.3, and the crosslinking ratio of the core of PVA II. However, it is possible that the shell, due to its already crosslinked state, will behave differently during the second crosslinking stage. This aspect will be examined later in this article.

### Polymer Characterization

The structural parameters of composite PVA II beads, as a function of the core crosslinking ratio, were characterized by swelling measurements at 37°C. The results (with  $n = 3$ ) are summarized in Table I, where  $Q$ , the equilibrium volume swelling ratio defined as the ratio of swollen to dry PVA volume, is equivalent to the reciprocal of the polymer volume fraction  $v_2$ . The number average mol wt between crosslinks,  $M_c$ , was calculated from a Flory–Rehner-type equation for highly crosslinked networks<sup>14</sup>:

$$\frac{1}{M_c} = \frac{2}{M_n} - \frac{v[\ln(1 - v_2) + v_2 + \chi v_2^2](1 - v_2^{2/3}/N)^3}{V_1(v_2^{1/3} - v_2/2)(1 + v_2^{1/3}/N)^2} \quad (2)$$

where  $M_n$  is the number average mol wt of the polymer before crosslinking,  $\chi$  is the Flory interaction parameter for the PVA-water system,  $v$  the specific volume of PVA ( $= 0.788 \text{ cm}^3/\text{g}$ ), and  $V_1$  the mol vol of the swelling solvent ( $= 18 \text{ cm}^3/\text{mol}$ ). The parameter  $N$  is the number of chain links defined by:

$$N = 2M_c/M_r \quad (3)$$

where  $M_r$  is the mol wt of the vinyl alcohol repeating unit ( $= 44$ ). For our calculations, a value of  $\chi = 0.7$  was used for the PVA-water system (37°C) in the present polymer volume fraction range of 0.426–0.599. This is consistent with  $\chi$  values of 0.7–0.8,

reported by Yano,<sup>15</sup> based on vapor phase sorption data at 30°C for the same range of polymer volume fractions. Previously, Peppas and Merrill<sup>16</sup> reported  $\chi$  values for the PVA–water system with low polymer volume fractions ( $v_2 < 0.12$ ). Extrapolation of their data to the present polymer volume fractions gives a  $\chi$  value at 30°C close to 0.6. Therefore, the choice of  $\chi = 0.7$  for a higher temperature of 37°C in the present analysis is reasonable in view of the results of Yano and those of Peppas and Merrill.

Also reported in Table I is the mesh size  $\xi$ , which represents the maximum size of diffusing species that can pass through the polymer network and, therefore, provides an indication of the screening effect of the network on solute diffusion. The following equation for determining  $\xi$  was utilized, which was based on the consideration of the end-to-end distance of polymer chains in the unperturbed (solvent-free) state<sup>17</sup>:

$$\xi = v_2^{-1/3}(Nl^2C_n)^{1/2} \quad (4)$$

where  $l$  is the C—C bond length ( $= 1.54 \text{ \AA}$ ) and  $C_n$  the Flory characteristic ratio or rigidity factor ( $= 8.9$  for PVA).

Equation (2) and its extensions have been successfully applied by Peppas et al.<sup>18</sup> to the characterization of highly crosslinked PHEMA hydrogels. It was shown that when  $M_n$  exceeds 10,000, the effect of  $M_n$  on  $M_c$  in eq. (2) is minimal. In the present study, a similar approach was adopted for the PVA gel beads by assuming  $M_n$  is sufficiently large so that the term  $2/M_n$  may be neglected. This assumption is valid in view of the viscosity average mol wt of about 150,000 obtained for the present PVA system based on methods described in the Experimental section. Equation (2) was subsequently solved iteratively using the  $M_c$  value for  $N \rightarrow \infty$  as the initial estimate.

From Table I, it is evident that as the core PVA crosslinking ratio  $X_c$  increases from 0.05 to 0.2, the

**Table I** Structural Parameters of Composite PVA Beads at 37°C

$X_c$ (mol/mol)	$v_2^a$	$Q$	$M_c$	$\xi$ (Å)
0.05	$0.426 \pm 0.012$	2.349	5940	100
0.10	$0.492 \pm 0.016$	2.032	860	36
0.17	$0.567 \pm 0.07$	1.863	350	22
0.20	$0.599 \pm 0.026$	1.669	270	19
0.20 <sup>b</sup>	$0.575 \pm 0.011$	1.740	320	21

<sup>a</sup> Mean  $\pm$  SD ( $n = 3$ ).

<sup>b</sup> With outer shell removed.

mol wt between crosslinks  $M_c$  decreases from 5940 to 270 (equivalent to from 135 to 6 repeating units), and the mesh size reduces from 100 to 19 Å. These results are consistent with data reported by Canal and Peppas<sup>17</sup> and by Gander et al.<sup>19</sup> on PVA crosslinked with glutaraldehyde. Since most of the  $M_c$  values in Table I are too small (less than 100 repeating units) to allow the assumption of a Gaussian distribution of the chain length between crosslinks, the utilization of eq. (2), which was obtained by Lucht and Peppas<sup>14</sup> for highly crosslinked networks with the assumption of Gaussian distribution relaxed, is therefore justified.

Table I also includes data from a PVA core with  $X_c = 0.2$  without the outer shell. The shell was carefully removed from a swollen PVA II bead by first puncturing the shell with a razor, followed by peeling slowly to separate it from the core. A comparison of results on PVA II beads ( $X_c = 0.2$ ), with and without the outer shell, suggests that the thin shell (about 21  $\mu\text{m}$ ) affects very little of the measured bulk polymer properties. For example, only about a 4% difference in  $v_2$  or  $Q$  is found when one evaluates structural characteristics of bulk PVA using swelling data of the present composite PVA beads.

#### Dynamic Swelling and Solute Release: Effect of Crosslinking Ratio

The effect of crosslinking ratio on the release of proxyphylline from dehydrated PVA II beads is shown in Figure 5 for a constant proxyphylline loading of 9.7%. The corresponding dynamic swelling behavior, in terms of the solvent front penetration, is presented in Figure 6, and that of the tran-

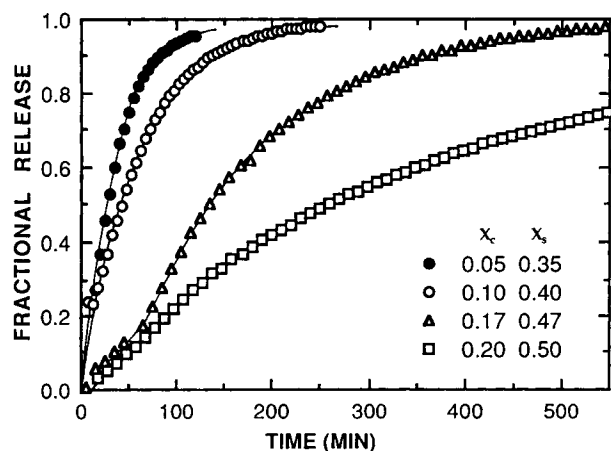


**Figure 5** Effect of crosslinking ratio on proxyphylline release from composite PVA II beads: 9.7% loading at 37°C.

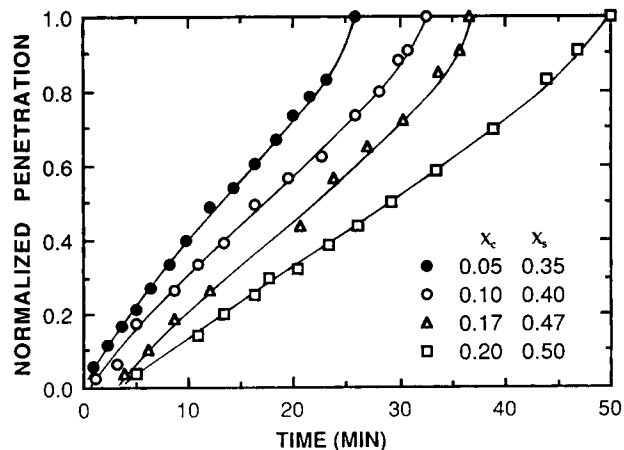


**Figure 6** Effect of crosslinking ratio on the swelling front movement in composite PVA II beads during proxyphylline release: 9.7% loading at 37°C.

sient dimensional changes appears in Figure 7 (shown with the bead diameter normalized to the equilibrium swollen diameter of the drug-free bead). It is evident from Figure 5 that the effect of crosslinking ratio on the release of proxyphylline is small at lower shell crosslinking ratios ( $X_s \leq 0.4$ ), where the reduction of network mesh sizes does not significantly affected the transport resistance, and the solute release generally is complete within 1–2 h. At these low crosslinking ratios, the associated release profiles are first order in nature, due to a combined effect of matrix diffusion and spherical geometry. On the other hand, at a shell crosslinking ratio of  $X_s \geq 0.47$ , the fractional solute release exhibits an initial time lag of up to 15 min, followed by a constant-rate (or linear) region of 2–3 h, before levelling

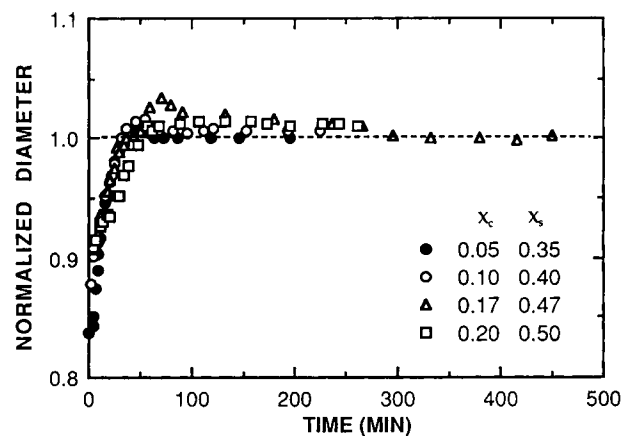


**Figure 7** Effect of crosslinking ratio on the transient dimensional changes during proxyphylline release from composite PVA II beads: 9.7% loading at 37°C.

off in a first-order fashion. The overall duration of solute release, in this case, is extended to more than 10 h. Such release behavior suggests that, at higher crosslinking ratios, the outer PVA shell initially functions as a rate-controlling membrane characterized by a diffusional time lag. Later, as solute release proceeds, the transport resistance through the core PVA matrix increase steadily as a result of increasing diffusional distance, which eventually exceeds the transport resistance through the outer shell. This results in the observed first-order release behavior during the latter part of the solute release.

The dynamic swelling results of Figure 6 show that, at a proxyphylline loading of 9.7%, the solvent front penetration during solute release is slower at higher PVA crosslinking ratios due to the increasing transport resistance at reduced network mesh sizes. In this case, the solvent front is also the glassy/rubbery swelling front, since all studies were carried out with dehydrated PVA II bead samples. Some Fickian contribution is evident from the slight non-linearity at the initial stage of the solvent front penetration. This is followed by a linear penetration region and, eventually, an accelerated penetration near the center. Such an apparent acceleration of solvent front penetration has been shown to be a natural outcome of the spherical geometry.<sup>9,20</sup> Similar to the release results of Figure 5, initial time lags in solvent front penetration are also observed in Figure 6 with shell crosslinking ratios of  $X_s \geq 0.47$ . The fact that the time lag for solvent front penetration is shorter (2–3 min) than that for the release of proxyphylline (10–15 min) suggests that the diffusion coefficient of water in the crosslinked PVA shell is several times higher than that of proxyphylline, due to the smaller molecular size of water and the inverse proportionality of the diffusion coefficient  $D$  to the time lag at a given membrane thickness.

It is worth noting that only less than 10% of the proxyphylline has been released (Fig. 5) at the time of completion of water penetration in solute-loaded PVA II beads (Fig. 6). Under such a condition, it is reasonable to expect that the solute distribution has not been significantly perturbed and is nearly constant throughout the PVA core during most of the initial swelling phase. This allows the analysis of the initial solute diffusion from such a membrane-matrix combination as a membrane-reservoir problem, at least approximately. With this approach, the apparent solute diffusion coefficient in the outer PVA shell is estimated from the following time-lag relationship for spherical geometry<sup>21</sup>:

$$t_L = \frac{l^2}{6D_s} \quad (5)$$

where  $t_L$  is the measured time lag,  $l$  is the shell thickness, and  $D_s$  is the apparent solute diffusion coefficient in the PVA shell. Equation (5) has the same form as the time-lag relationship for the sheet geometry. The apparent solute diffusion coefficient in the PVA core is obtained from the following large-time approximation to the solution of Fickian diffusion equation for spheres<sup>22</sup>:

$$\frac{M}{M_\infty} = 1 - \frac{6}{\pi^2} \exp(-D_c \pi^2 t/a^2) \quad (6)$$

where,  $M/M_\infty$  is the fractional release,  $D_c$  is the apparent solute diffusion coefficient in the PVA core, and  $a$  is the radius of the bead. By plotting  $\ln(1 - M/M_\infty)$  vs.  $t$ ,  $D_c$  is evaluated from the slope.

Utilizing both eqs. (5) and (6), apparent diffusion coefficients of proxyphylline in the PVA shell and core have been calculated from the data of Figure 5 and have been summarized in Table II. It is apparent that, at higher crosslinking ratios, the proxyphylline diffusion coefficient in the outer PVA shell is about one order of magnitude smaller than that in the core. This is again attributed to the more pronounced decreases in the corresponding mol wt between crosslinks and the associated reduction of network mesh sizes in the shell. It is also interesting to note that, when going from  $X_c = 0.17$  to 0.20, the proxyphylline diffusion coefficient in the core ( $D_c$ ) decreases by a factor of 4, whereas that in the shell ( $D_s$ ) decreases by a factor of 3 or so. This suggests a slight deviation from the additivity of crosslinking ratios in the shell of PVA II as alluded to earlier in this article. Such deviation can become large when the crosslinking ratios of the present PVA II core and shell are increased further, such that the access to crosslinking

**Table II Diffusion Characteristics of Proxyphylline in Composite PVA Beads\* (37°C): Effect of Crosslinking**

$X_s$ (mol/mol)	$X_c$ (mol/mol)	$D_s \times 10^9$ (cm <sup>2</sup> /sec)	$D_c \times 10^9$ (cm <sup>2</sup> /sec)
0.35	0.05	—	189
0.40	0.10	—	107
0.47	0.17	2.5	44.5
0.50	0.20	0.8	11.3

\* 9.7% proxyphylline loading.



sites in the shell is significantly more restricted than that in the core.

At a fixed solute loading of 9.7%, the transient dimensional changes during the simultaneous water penetration and proxyphylline release do not seem to be significantly affected by the crosslinking ratios (Fig. 7). In all cases, the swelling bead diameter goes through a broad maximum, followed by a gradual approach to an equilibrium value, where the approach to such swelling equilibrium becomes slower at higher crosslinking ratios. The maximum bead diameter appears to be less sensitive to variations in crosslinking ratios. In contrast, as will be shown later, the maximum bead diameter of the present composite PVA system is more sensitive to solute loading levels.

### Dynamic Swelling and Solute Release: Effect of Loading Level

The effect of loading on the release of proxyphylline from PVA II beads with  $X_c = 0.17$  and  $X_s = 0.47$  is presented in Figure 8 for loading levels up to 25.3%. The corresponding water penetration behavior is shown in Figure 9, and that of the transient dimensional changes in Figure 10. As with other hydrophilic polymers, the proxyphylline release rate from the present composite PVA system increases with increasing solute loading (Fig. 8). The release time lag, due to the surface membrane effect, appears to decrease slightly at higher solute loadings, whereas the time lag for water penetration is relatively insensitive to solute loadings (Fig. 9). Similar to Fig-

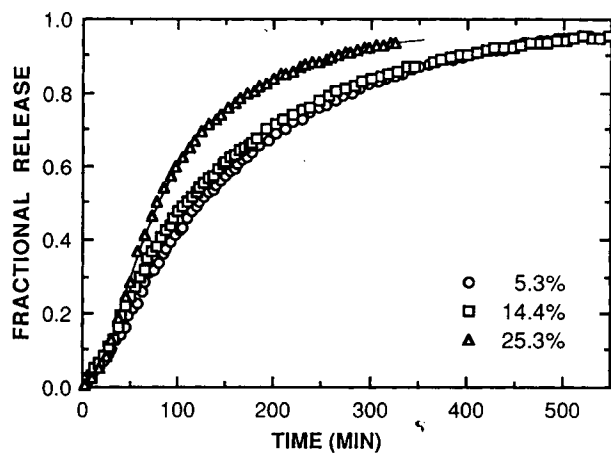


**Figure 8** Effect of loading level on proxyphylline release from composite PVA II beads:  $X_c = 0.17$ ,  $X_s = 0.47$  at 37°C.

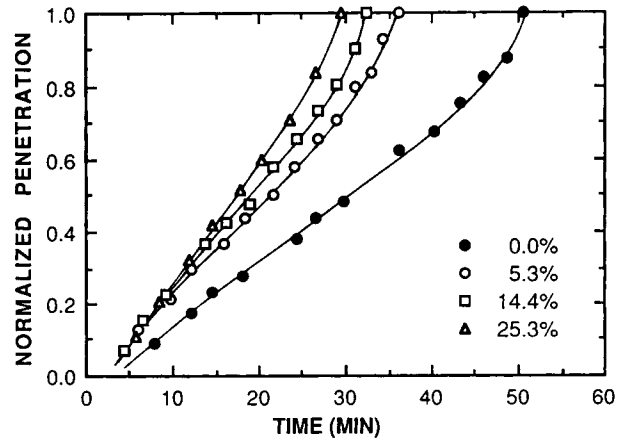


**Figure 9** Effect of loading level on the swelling front movement in composite PVA II beads during proxyphylline release:  $X_c = 0.17$ ,  $X_s = 0.47$  at 37°C.

ure 6, the results of Figure 9 on the swelling front penetration show the anticipated kinetic behavior for spherical samples.<sup>9,20</sup> Based on eqs. (5) and (6), diffusion coefficients of proxyphylline in the PVA shell and core have been evaluated from the data of Figure 8 and summarized in Table III. Similar to data shown in Table II, the proxyphylline diffusion coefficients in the PVA shell are also observed to be about one order of magnitude smaller than that in the core. Furthermore, the concentration dependence of proxyphylline diffusion coefficients in the PVA shell is evident from their increasing trend with the solute loading. However, such a trend is less obvious for proxyphylline diffusion coefficients in the PVA core.

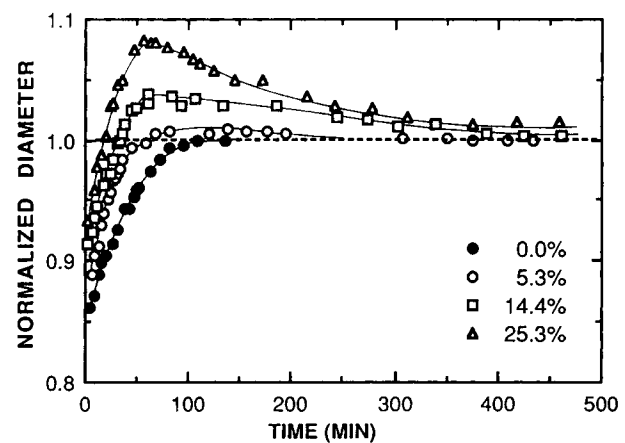


**Figure 10** Effect of loading level on the transient dimensional changes during proxyphylline release from composite PVA II beads:  $X_c = 0.17$ ,  $X_s = 0.47$  at 37°C.

**Table III Diffusion Characteristics of Proxyphylline in Composite PVA Beads\* (37°C): Effect Loading Level**

Proxyphylline Loading (%)	$D_s \times 10^9$ (cm <sup>2</sup> /sec)	$D_c \times 10^9$ (cm <sup>2</sup> /sec)
5.3	1.9	39.1
9.7	2.5	44.5
14.4	3.1	31.9
25.3	4.1	48.7

\*  $X_s = 0.47$ ;  $X_c = 0.17$ .

The transient dimensional changes of Figure 10, observed during solvent penetration and proxyphylline release, exhibit a more pronounced maximum at higher solute loadings as compared with the monotonic increase in bead size in the solute-free PVA II. In fact, the maximum bead size increases, whereas the time to reach the maximum decreases, with increasing levels of proxyphylline loading. It should be pointed out that when the normalized bead diameter reaches a maximum, the corresponding fractional solute release is still less than 30% (Fig. 8). This contrasts the 70–80% solute release at peak swelling during the release of water soluble compounds from poly(hydroxyethyl methacrylate) (HEMA) based hydrogel beads.<sup>8</sup> In the present case, although proxyphylline is also water soluble, the presence of a rate-controlling shell in PVA II retards solute diffusion while permitting rapid water transport. This results in the reduced extent of solute release at the swelling maximum. In addition to the general scheme of kinetic events, leading to the observed swelling maximum, the effects of solute solubilities as well as the contribution from osmotic forces have recently been investigated in detail in the HEMA-based copolymer bead system.<sup>9</sup> It is believed that the local presence of a solute in the hydrophilic polymer generates an additional osmotic driving force (in addition to the polymer swelling osmotic force), which can change both the total swelling pressure and the associated time-dependent relaxation behavior of the hydrogel network during the simultaneous absorption of water and the release of the solute. Although the observed maximum in the transient dimensional changes intuitively can be attributed to a combination of two competing processes, namely the reduction of bead size due to solute release and the increase in bead size due to polymer swelling, the osmotic contribution from the solute will play a significant role when contributions from such competing processes are small. In this

situation, the osmotic contribution from the solute loading continues to build up during the initial stages of the polymer swelling and solute dissolution. After the completion of solvent penetration, the internal solute concentration, and hence its role in the osmotic contribution, declines continuously as the release proceeds. In response to such a change in total swelling osmotic pressure, the swollen diameter of the hydrogel bead goes through a maximum. Since such an osmotic contribution from the solute increases with solute loading, the corresponding maximum bead size will therefore increase accordingly.

## CONCLUSION

A new method of preparing large spherical PVA beads (up to 1.5 mm in diameter) with a core-shell structure has been developed. This is achieved by a stepwise saponification of suspension polymerized PVAc beads, followed by a stepwise crosslinking of the PVA core and shell with glutaraldehyde. The characterization of polymer structure, as well as the swelling and solute release kinetics, was studied as a function of PVA crosslinking ratio and solute loading using proxyphylline as a model compound. The results show that the outer PVA shell functions as a rate-controlling membrane upon increasing its crosslinking ratio,  $X_s$ , above 0.47, as characterized by the observed diffusional time-lags and constant-rate regions during solute release. The effect of the crosslinking is also reflected in the corresponding decrease of proxyphylline diffusion coefficients in both the PVA shell and core at increasing crosslinking ratios. At a fixed crosslinking ratio, some concentration dependence has been observed for the proxyphylline diffusion coefficients in the PVA shell, but not in the core. The composite PVA beads reported here are potentially useful as drug carriers or absorbent for separation purposes.

This work was supported by grants from the Medical Research Council of Canada and the Ontario Centre for Materials Research.

## REFERENCES

1. S. H. Gehrke, G. P. Andrews, and E. L. Cussler, *Chem. Eng. Sci.*, **41**, 2153 (1986).
2. L. Brannon-Peppas and R. S. Harland, Eds., *Absorbent Polymer Technology*, Elsevier, Amsterdam, 1990.
3. S. H. Gehrke and P. I. Lee, in *Specialized Drug Delivery Systems*, P. Tyle, Ed., Marcel Dekker, New York, 1990, pp. 333–392.

4. P. I. Lee, *J. Controlled Release*, **2**, 277 (1985).
5. R. W. Korsmeyer and N. A. Peppas, *J. Membrane Sci.*, **9**, 211 (1981).
6. P. Colombo, A. Gazzaniga, C. Caramella, W. Conte, and A. Lamanna, *Acta Pharm. Technol.*, **33**, 15 (1987).
7. B. Gander, V. Beltrami, R. Gurny, and E. Doelker, *Int. J. Pharm.*, **58**, 63 (1990).
8. P. I. Lee, *Polym. Commun.*, **24**, 45 (1983).
9. P. I. Lee and C.-J. Kim, *J. Controlled Release*, **16**, 229 (1991).
10. C.-J. Kim and P. I. Lee, *Polym. Mater. Sci. Eng.*, **63**, 64 (1990).
11. D. N. Mead and R. M. Fuoss, *J. Am. Chem. Soc.*, **63**, 2832 (1941).
12. C. A. Finch, Ed., *Poly(Vinyl alcohol): Properties and Applications*, Wiley, New York, 1973.
13. C. Hirayama, K. Kawaguchi, and Y. Motozato, *J. Chem. Soc. Jpn.*, **1974**, 894 (1974).
14. L. M. Lucht and N. A. Peppas, in *Chemistry and Physics of Coal Utilization*, B. S. Cooper and L. Petrakis, Eds., American Institute of Physics, New York, 1981, pp. 28-48.
15. Y. Yano, *J. Chem. Soc. Jpn.*, **76**, 668 (1955).
16. N. A. Peppas and E. W. Merrill, *J. Polym. Sci. Polym. Chem. Ed.*, **14**, 459 (1976).
17. T. Canal and N. A. Peppas, *J. Biomed. Mater. Res.*, **23**, 1183 (1989).
18. N. A. Peppas, H. J. Moynihan, and L. M. Lucht, *J. Biomed. Mater. Res.*, **19**, 397 (1985).
19. B. Gander, R. Gurny, E. Doelker, and N. A. Peppas, *Pharm. Res.*, **6**, 578 (1989).
20. P. I. Lee and C.-J. Kim, *J. Membrane Sci.*, **65**, 77 (1992).
21. W. R. Good and P. I. Lee, in *Medical Applications of Controlled Release*, Vol. I, R. S. Langer and D. L. Wise, Eds., CRC Press, Boca Raton, FL, 1984, pp. 1-82.
22. J. Crank, *The Mathematics of Diffusion*, Oxford University, London, 1975, p. 91.

Received October 7, 1991

Accepted January 12, 1992